

## Analisis of Corrosion Behavior of Ti-15Mo Alloys

C.G. Nava-Dino<sup>1, 5</sup>, R. G. Bautista-Margulis<sup>2</sup>, M. A. Neri-Flores<sup>1</sup>, M. V. Orozco-Carmona<sup>1</sup>,  
S.D de la Torre<sup>3</sup>, J.G. Gonzalez-Rodriguez<sup>4</sup>, J. G. Chacon-Nava<sup>1</sup> and A. Martínez-Villafañe<sup>1,\*</sup>

<sup>1</sup> Departamento de Integridad y Diseño de Materiales Compuestos. Centro de Investigación en Materiales Avanzados. S.C. CIMAV. Miguel de Cervantes No. 120, Complejo Industrial Chihuahua, C.P 31109, Chihuahua, Chihuahua, México.

<sup>2</sup> Universidad Juárez Autónoma de Tabasco, División Académica de Ciencias Biológicas, C.P. 86040, Villahermosa, Tabasco, México.

<sup>3</sup> Centro de Investigación e Innovación Tecnológica (CIITEC)-IPN, D.F. México, Cerrada de Cecati S/N, Col. Santa Catarina Azcapotzalco, CP 02250, México D.F.

<sup>4</sup> Centro de Investigación en Ingeniería y Ciencias Aplicadas-UAEM, Av. Universidad 1001, Col. Chamilpa, 62210-Cuernavaca, Morelos, MEXICO.

<sup>5</sup> Universidad Autónoma de Chihuahua, Facultad de Ingeniería, Chihuahua, Chih. México.

\*E-mail: [martinez.villafañe@cimav.edu.mx](mailto:martinez.villafañe@cimav.edu.mx)

Received: 22 February 2012 / Accepted: 7 April 2012 / Published: 1 May 2012

---

The Ti-15Mo alloys have been studied by using electrochemical measurements. The electrochemical test was made to analyze their resistance and predictability to corrosion from green dust samples, SPS samples and arc-melt alloying. The corrosion behavior in Ringer's solution was evaluated by Potentiodynamic polarization curves, electrochemical noise and SEM (Scanning Electron Microscope). Images were used to study corrosion behavior and corrosion predictability.

---

**Keywords:** Electrochemical measurements, Ringer's Solution, Mechanical alloying, SPS, arc-melt.

### 1. INTRODUCTION

In recent years titanium alloys, particularly the Ti–Mo alloys have received considerable attention as a biomaterial since they offer significant benefits in terms of corrosion resistance and mechanical biocompatibility. Ti–Mo alloys as a suitable biomaterial due to their ability to exhibit spontaneous passivation, better electrochemical stability of the passive films formed on that and their excellent biocompatibility [1]. The corrosion resistance of titanium alloys depends on the factors such as composition microstructure and environment [2].

Titanium undergoes an allotropic transformation, changing from the high temperature  $\beta$  phase (body-centered cubic structure) to  $\alpha$  phase (hexagonal close-packed structure) upon cooling. Alloying elements are classified as  $\alpha$  or  $\beta$  stabilizers depending on their effect on the transformation temperature, or  $\beta$  transus. Al is the most commonly used element to stabilize  $\alpha$  phase to higher temperatures, although it also has significant solubility in the  $\beta$  phase for V, Mo, and Nb [3].

The purpose of this study is to investigate the effects of milling time and sintering process and corrosion behaviour in Ti-15Mo. Corrosion resistance was also evaluated by performing polarization tests and electrochemical noise (EN) test were repeated at least three times for each condition. The interpretation of data from electrochemical noise and potentiodynamic polarization studies were analyzed and related to multifractal wavelet modeling.

## 2. MATERIALS AND METHODS

### 2.1 Materials and experimental procedure

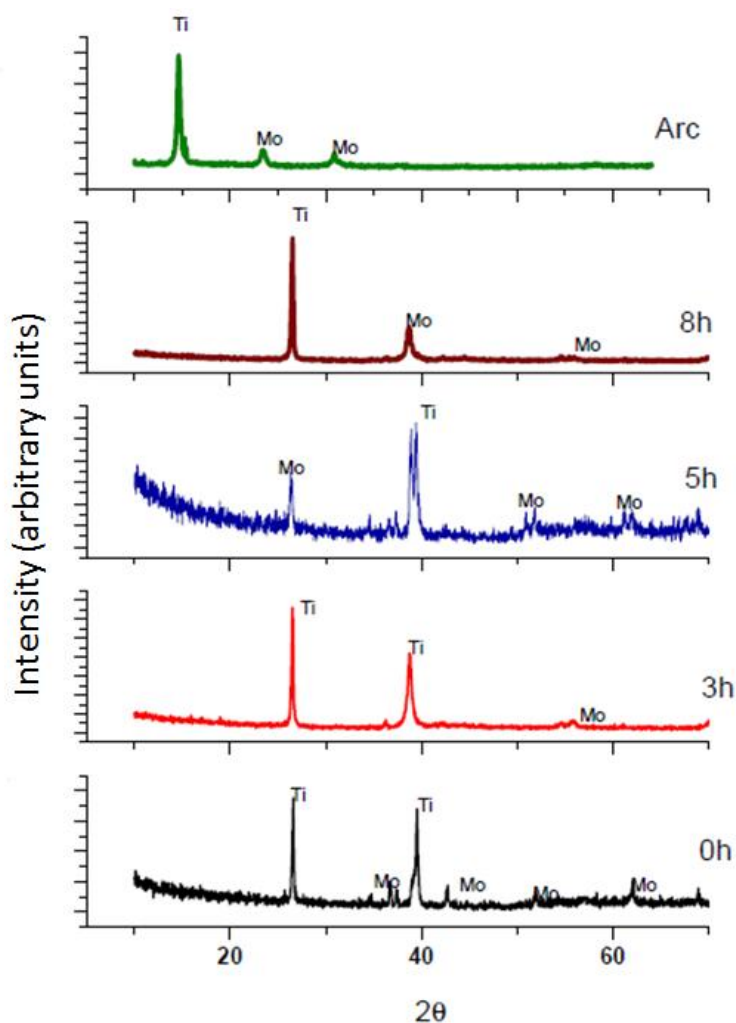


**Figure 1.** X-ray diffraction pattern of the Ti-15Mo samples 0, 3, 5, 8 h made by SPS and arc-melt.

Pure materials from Alfa Aesar were used: titanium (99.5% purity), molybdenum (99.5%) powders. The first step was the preparation by milling with the corresponding quantity of metal powder in a high energy SPEX 8000M connected a hardened steel container with 13mm(Ø) balls as milling media and an inert Ar atmosphere.

The milling ball to powder weight ratio was kept 5 to 1 for all experimental runs. Methanol was used as process control agent (PCA-1 ml). Milling intervals were 0, 3, 5 and 8 h using alternate cycles of 30 min milling and 30 min resting to protect samples from overheating, using the same milling device for 1 h with the addition of 3 drops of methanol as PCA in order to avoid excessive agglomeration. Green (consolidated) products were obtained by pressing milled powders into a circular die at 950MPa under uniaxial load.

**Table 1.** Variation of microhardness of Ti-15Mo, made by SPS and arc-melt.

Milling intensity [h] SPS	Microhardness [Vickers]
0	167 Hv
3	129 Hv
5	123 Hv
8	327 Hv
Arc-melt	526 Hv

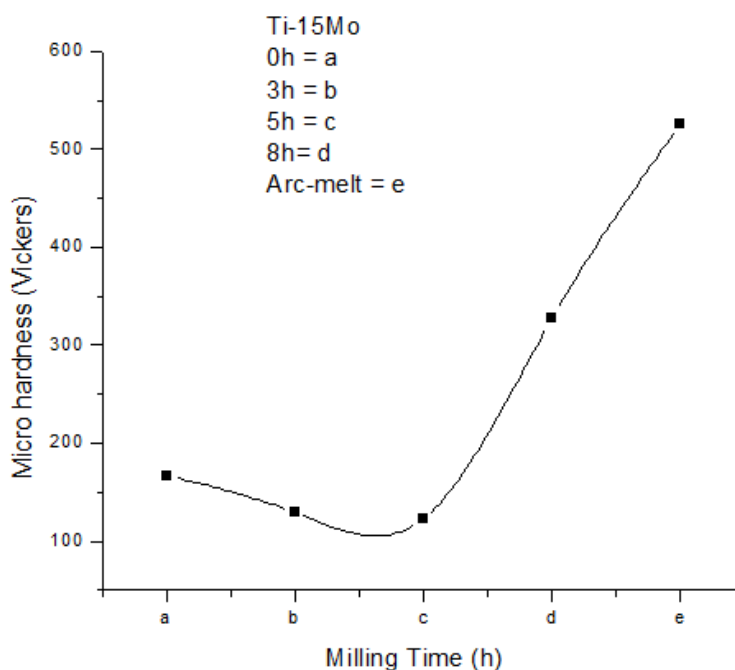


**Figure 2.** Microhardness Ti-15Mo with milling time for samples sintering by SPS and arc-melt.

The diffraction profiles were measured by a Philips X'pert powder diffractometer using a Cu cathode (= 0.15406 nm). The step size and step time were 0.0334 and 50 s, respectively. X-ray

diffraction peak profile analysis was carried out to determine the crystallite size. Microstructural observations were performed by using a transmission electron microscope TEM (Philips JEM-2200FS) equipped with energy dispersive spectrometer (EDS). The differences between SPS milling time and arc-melt are showing in figure 1. Afterwards, pressed samples were mounted and polished with standard metallographic techniques in order to carry out the microstructural observations by using a scanning electron microscope JEOL-5800-LV. Hardness tests were carried out in a Wilson Rockwell Instron hardness meter, obtaining values in Vickers scale, as shown in table 1. Chart average value of 3 indentations and its standard error were present. Figure 2 shows microhardness of Ti-15Mo 0, 3, 5, 8 h SPS and arc-melt.

## 2.2 Preparation of the simulated biofluids

Alloy used in this study was in the form of bottom of a 5g powder, with composition of Ti, 15Mo in balance. The Ti-15Mo rod was polished (Silicon carbide paper 1200). The total surface of the electrode of Ti-15Mo was coated with epoxy resin. The electrode was rinsed in Ringer's solution. The Ringer's solution has a chemical composition (in g/l) 9NaCl, 0.24 CaCl<sub>2</sub>, 0.43 KCl and 0.2 NaHCO<sub>3</sub> to distilled water. This electrolyte was intended to simulate surgical implant conditions [4-5]. Electrochemically, titanium alloys have high resistance as a result of their very stable oxide films formed by titanium dioxide (TiO<sub>2</sub>), which is the most stable oxide of titanium, and some suboxides. The physiological and electrochemical properties of titanium dioxide film and its long-term stability in biofluids play an important role for the biocompatibility of titanium and its implant alloys [6].

## 2.3 Morphological characterization

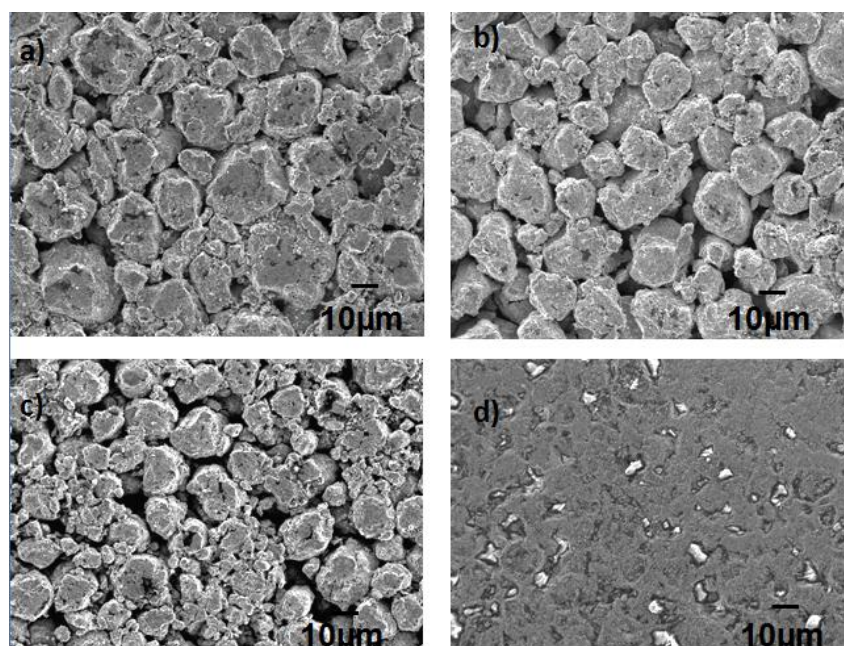


**Figure 3.** SEM micrograph of Ti-15Mo green powders milled for (a) 0, (b) 3, (c) 5 and (d) 8h; before SPS sintering.

The surface morphology of the samples was previously analyzed by using scanning electron microscope (SEM). After that samples were immersed in Ringer's solution a) 0, b) 3, c) 5 and d) 8 hours of milling time, as illustrated in figure 3. The reduction of size is observed as milling hours are increased. Before applying the electrochemical test, SPS sintering samples in 0, 3, 5 and 8h were observed (see figure 4). These samples were clean and polished to see their composition.

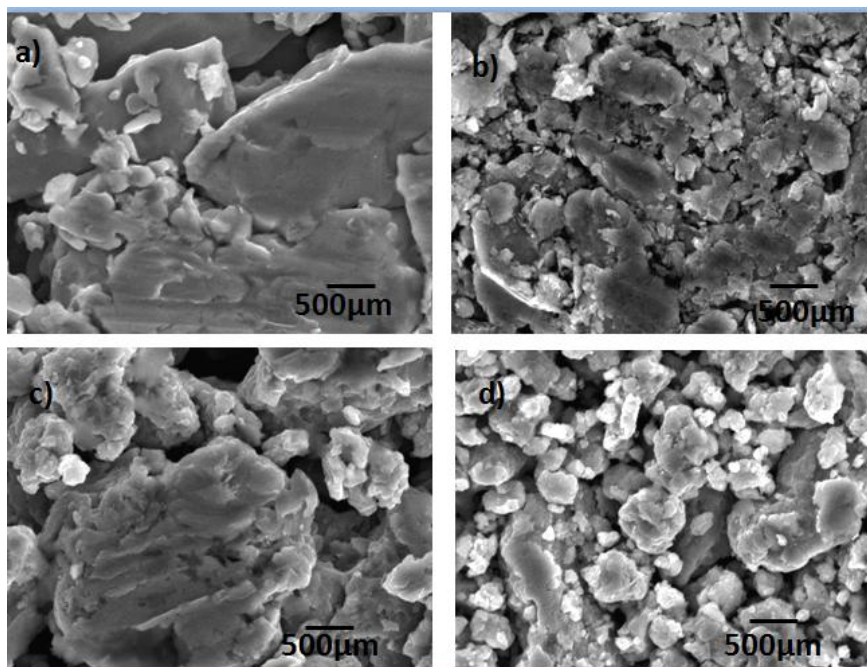


**Figure 4.** Ti-15Mo clean samples sintering by SPS at (a) 0, (b) 3, (c) 5 and (d) 8h before noise and potentiodynamic test.

To investigate the microstructural changes in the Ti–15Mo alloys, some studies related that, corrosion resistance of titanium alloys depends on such factors as microstructure, composition and environment [7].

#### 2.4 Electrochemical characterization

Titanium cannot be used directly; an oxide layer on the metal surface can be using several ways as chemical, electrochemical, thermal treatment, and anodization methods, among others [8]. Some researchers consider an important factor involved in the process of corrosion, is the temperature, because the corrosion rate increases as the temperature increase in the corrosion medium on the reactions proceeding in pure acids [9].

In this research, an electrochemical test of Ti-15Mo samples was performed. Such samples were immersed in Ringer's solution for half an hour for stabilization and the open circuit potential was measured during this period with a multimeter; the OCP samples were -389 and -226 mV vs SCE for 0 to 8 h milling an arc-melt alloying. All tests were performed by  $\pm 37$  °C; this temperature was used to

simulate human body temperature. The electrochemical corrosion behavior in cyclic polarization and electrochemical noise (EN) were performed. In the past 40 years, electrochemical noise (EN) technique has received more and more interest in both laboratory and field applications for its non-disturbance and sensitivity to localized corrosion monitoring. One of the most important things for EN technique is to choose an appropriate method to analyze EN records to obtain the related corrosion information [10]. The Densities of nanometric samples of Ti-15Mo made by SPS and arc-melt can be seen in table 2.

**Table 2.** Densities of nanometric samples of Ti-15Mo made by SPS and arc-melt.

Milling intensity [h] SPS	Density
0	3.8006 ± 0.061 g/cc
3	3.8674 ± 0.017 g/cc
5	3.9248 ± 0.021 g/cc
8	3.9739 ± 0.073 g/cc
Arc-melt	4.1230 ± 0.003 g/cc

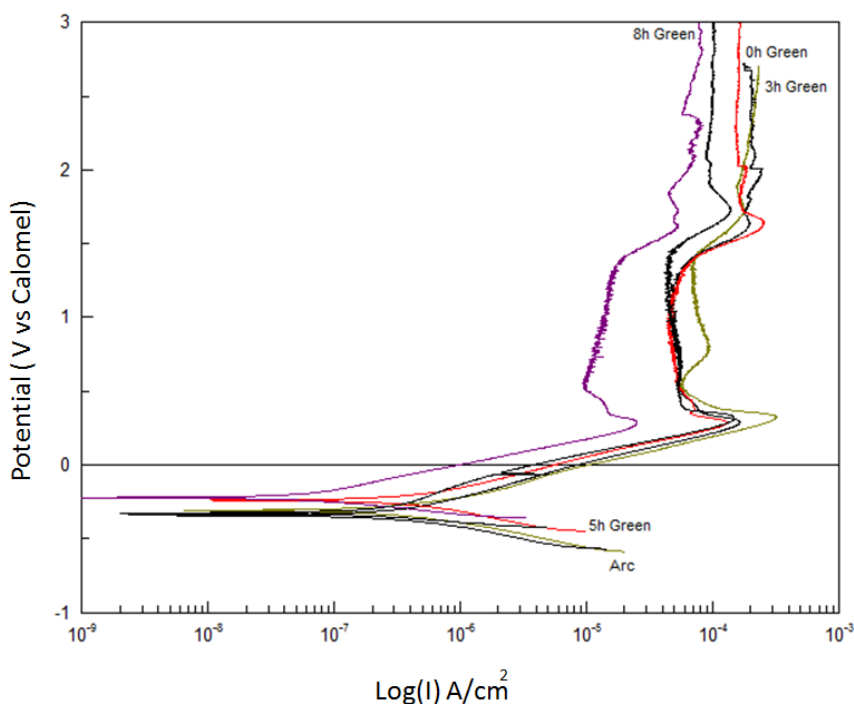


**Figure 5.** Ti-15Mo green samples in potentiodynamic test under Ringer's solution.

For comparison linear polarization curves were obtained, a typical three electrode arrangement was used with a saturated calomel reference electrode. The potentiodynamic polarization curves of Ti-15Mo in Ringer's of 0, 3, 5 and 8 h are shown in figure 5. The reverse scan curve of all the four different samples indicates their high resistance to pitting corrosion in Ringer's solution. The

electrochemical noise measurements were made recording simultaneously the potential and current fluctuations at a sampling rate of 0.7 point per second for a period of 2048 seconds. The corrosion products obtained by potentiodynamic polarization curves are observed in figure 6, corrosion products by EN are shown in figure 7.

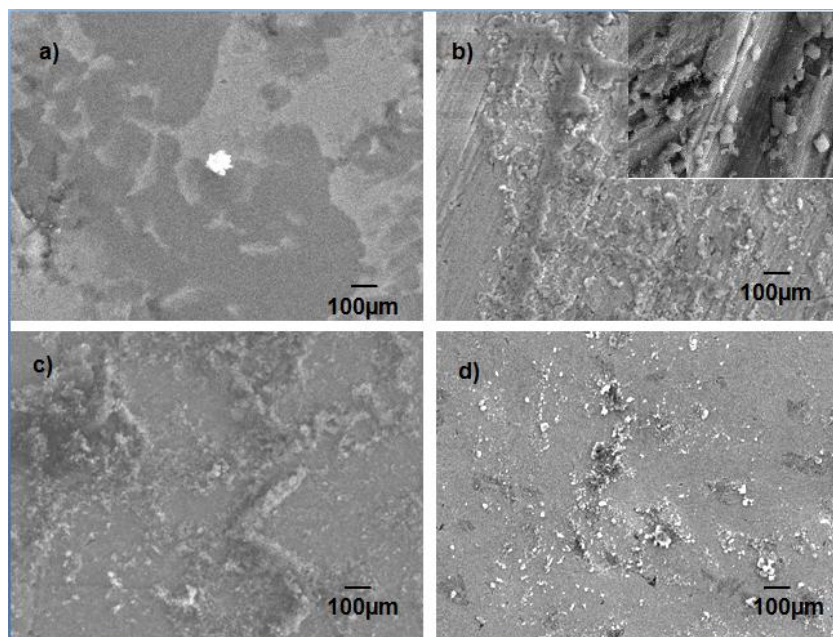


**Figure 6.** Ti-15Mo SPS samples at (a) 0, (b) 3, (c) 5 and (d) 8h after potentiodynamic in ringers solution.

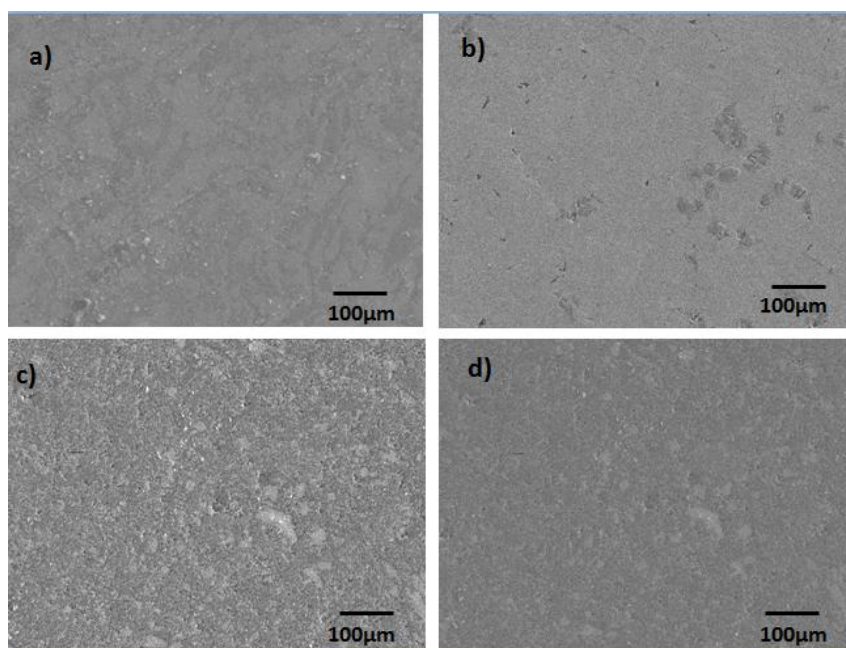


**Figure 7.** Ti-15Mo SPS samples at (a) 0, (b) 3, (c) 5 and (d) 8h after electrochemical noise (EN) in ringers solution.

For some studies electrochemical noise measurement analysis was showed as a powerful tool to monitor the morphology because EN technique is useful to obtain complementary information about samples [11]. In another cases the influence of the cathodic process reduces the amplitude of the EN signals and they arising from pitting corrosion on stainless steels are only measurable [12]. To understand the corrosion process in Ti-15Mo, signal analysis and images were used in several studies.

### 2.5 Signal and processing Images

Some studies have presented spectral analysis and FD (fractal dimension) to correlate the EEG (electroencephalogram) spectral characteristics. Complexity of a signal is determined by the corresponding FFT (Fast Fourier Transform) spectral profile [13]. Using the MATLAB image processing toolbox and selecting a ROI (Region of interest) in an image it was possible to obtain information from specimens [14].

In this research SEM images were taken for their analysis by the signal. This signal is received from the SEM image in order to have the feasibility of the two-dimensional image analysis. The MATLAB software was used to understand the corrosion behavior of the samples to corrosion predictability by electrochemical module. Correlations between signals from different techniques were studied. Correlations between EN, elongation and digital image correlation were used as a tool to know corrosion behaviour [15, 16].

## 3. RESULTS AND DISCUSSION

The results of microhardness are shown in table 1. Five indentations were made on each sample to obtain an average value of microhardness. The samples of higher hardness were observed at 8h. The graphics of microhardness were listed in figure 2. In this graphics, it was possible to see that microhardness was incremented during milling time of 3h and 8h. Table 2 shows that exists more microhardness index in 8h samples, than 3h and 5h. Microhardness test was made by green samples of materials with 5 grams of weight, and compacted in 5 seconds with 10 tons. The repeatability was performed with 5 indentations mounted in resin, after they were polished.

In general, the corrosion behavior of the samples reflects the changing corrosion conditions over the samples surface along the period of immersion in Ringer's solution. Results from digital image processing were obtained, under principles of morphological operations, to delimit the important regions in micrographs and allows to understanding the various changes on the surfaces of the samples.

The Ti-15Mo green samples in potentiodynamic test under ringer's solution has a good behaviour and does not shows big differences between them. In 3h is possible to see some little differences in  $I_{corr}$ , this could be because 0h is used as a white sample (see table 3). In sintered samples the signify changes are on 0h and arc melt,  $E_{corr}$  (V) because they was close similar in their values.

The corrosion type obtained from Electrochemical noise (EN) explain that in average corrosion was located and generalized.

**Table 3.** Electrochemical and dynamical parameters, under Ringer's solution.

Type of sample Ringer's Solution	$E_{\text{corr}}$ (V)	$I_{\text{corr}}$
Green 0h	-0.3412	5.7036E-7
Green 3h	-0.2989	9.0476E-8
Green 5h	-0.2171	2.3048 E-8
Green 8h	-0.2219	6.9952E-8
SPS 0h	-0.3787	2.7791E-7
SPS 3h	-0.2304	3.0153E-7
SPS 5h	-0.2660	1.1968E-6
SPS 8h	-0.3258	2.2664E-7
Arc-melt	-0.3798	2.3658E-7

X-ray diffraction pattern of the Ti-15Mo samples shows remarked differences in 5h SPS samples, this result coincide with electrochemical changes in  $I_{\text{corr}}$ . These observations could be related to the mechanical milling process, because 5h is a big change in milling hours from 0h who is only white sample. During the milling process 5h marks a most consolid alloying of Ti-15Mo. In table 2, these observations coincide with density values; they changes in 5h and then values were establish. This results coincide with another authors who explain that Ti-15Mo has a lot of changes and phases as result of alloying stabilizers; they usually tends to stabilize the  $\beta$  phase and to decrease the elastic modulus of the Ti alloys [17]. Also, molybdenum can be improved by reducing its grain size, stabilizes a small grain size during powder metallurgical (PM) manufacturing [18]. Corrosion results throws on the anodic phase, at sufficiently positive potentials, metal oxidation can take place while, on the cathodic phase, at sufficiently negative potentials, the cathodic reaction, for example oxygen reduction.[19, 20]

#### 4. CONCLUSIONS

- From the EDS analysis shown in figure 9, the Ti-15Mo samples presented their surface covered with O, Na, Cl as corrosion products.
- One possible reason for the corrosion behavior observed in Ti-15Mo green samples, SPS and sintering is that they are resistant to corrosion; because the oxide protective layer is independent of sintering or without sintering process.
- The  $E_{\text{corr}}$  and  $I_{\text{corr}}$  corrosion obtained and presented in table 3, and the high polarization resistance, are consistent with the corrosion noise behavior observed (see figure 8 and table 4). The

samples presented corrosion potentials and higher polarization resistant values, therefore good corrosion behavior.

- Ti-15Mo is a well known material and widely used for biological applications, with good corrosion properties as confirmed by the SEM micrographs and corrosion graphs.

- 

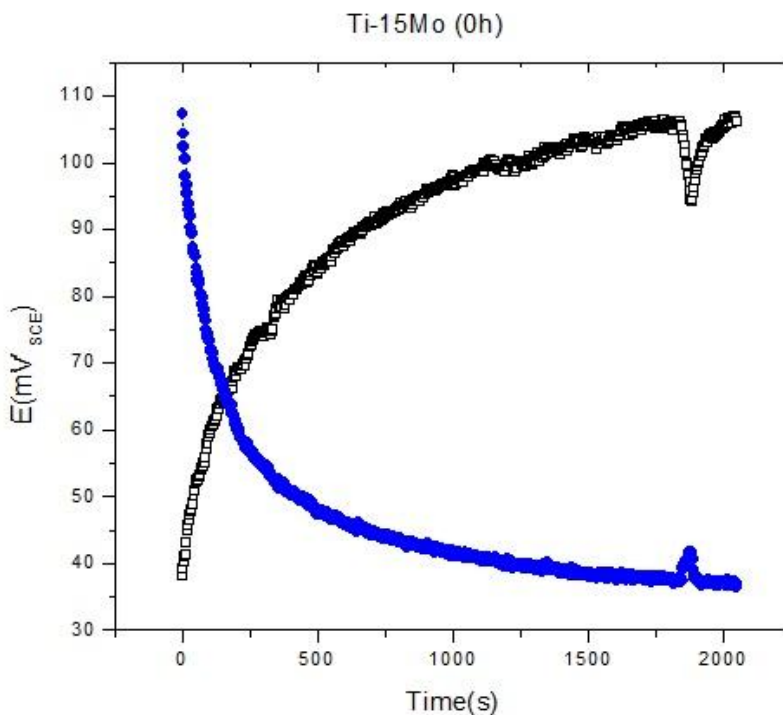


Figure 8. Electrochemical noise (EN), of Ti-15Mo 0h in Ringer's solution.

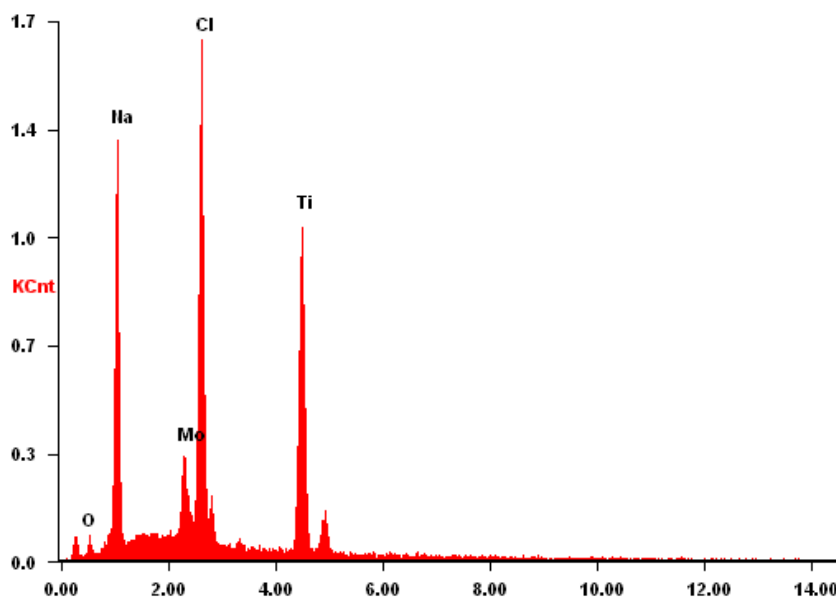


Figure 9. Corrosion products showed by EDS analysis.

**Table 4.** Electrochemical noise (EN) of Ti-15Mo

Specimen	R <sub>n</sub> (ohm.cm <sup>2</sup> )	Localization Index IL	Corrosion Type
Ti-15Mo SPS 0h	19699.06	0.2959	Located
Ti-15Mo SPS 3h	77667.17	0.5394	Located
Ti-15Mo SPS 5h	23157.01	0.3167	Located
Ti-15Mo SPS 8h	3820.25	0.0981	Mixed
Ti-15Mo Green 0h	7088.41	0.0726	Mixed
Ti-15Mo Green 3h	149576.90	0.0028	Generalized
Ti-15Mo Green 5h	1688.41	0.6959	Located
Ti-15Mo Green 8h	5.68089E-06	0.0037	Generalized
Ti-15Mo Arc	1446.06	0.2500	Located

#### ACKNOWLEDGMENTS

This research work was supported by Nanomining-263942 (FP7-NMP-2010-EU-MEXICO). The technical assistance by Adan Borunda, Enrique Torres, Karla Campos, Jair Lugo Cuevas and Gregorio Vazquez-Olvera is gratefully acknowledged.

#### References

1. S. Kumar, T.S.N.S. Narayanan, S. Saravana Kumar, *Corros. Sci.*, 52 (2010) 1721–1727.
2. X.H. Mina, S. Emuraa, N. Sekido, T. Nishimuraa, K. Tsuchiyaa, K. Tsuzakia, *Mater. Sci. Eng., A*, 527 (2010) 2693–2701.
3. M. Atapour, A.L. Pilchak, G.S. Frankel, J.C. Williams, *Mater. Sci. Eng., C*, 31 (2011) 885–891.
4. N.T.C. Oliveira, A.C. Guastaldi, *Acta Biomater.*, 5 (2009) 399–405.
5. H. Zohdi, H.R. Shahverd, S.M.M. Hadavi, *Electrochem. Commun.*, 13 (2011) 840–843
6. A.M. Fekry, and M.A. Ameer, *Int. J. Electrochem. Sci.*, 6 (2011) 1342 - 1354
7. F. Barragán, R. Guardián, C. Menchaca, I. Rosales, J. Uruchurtu, *Int. J. Electrochem. Sci.*, 5 (2010) 1799 – 1809
8. X.H. Min, S. Emura, T. Nishimura, L. Zhang, S. Tamilselvi, K. Tsuchiya, K. Tsuzaki, *Mater. Sci. Eng., A*, (2010) 1480–1488
9. E.M. Esparza Zúñiga, M.A. Veloz Rodríguez, J. Uruchurtu Chavarín, V.E. Reyes Cruz, *Int. J. Electrochem. Sci.*, 6 (2011) 5016 – 5030.
10. J.Y. Huang, Y.B. Qiu, X.P. Guo, *Electrochim. Acta.*, 54 (2009) 2218–2223
11. H. S. Klapper, J. Goellner, A. Heyn, *Corros. Sci.*, 52 (2010) 1362–1372
12. F. Safizadeh, A. Lafront, E. Ghali, G. Houlachi, *Hydrometallurgy* 111 (2012) 29–34
13. S. Spasic, A. Kalauzi, S. Kesic, M. Obradovic, J. Saponjic, *J. Theor. Biol.*, 289 (2011) 160–166
14. H. Suk Choi, J. HwanCheung, S. HyoKim, J. HeeAhn, *NDT and E Int.*, 44 (2011) 597–608
15. J. Kovac, C. Alaux, T. James Marrow, E. Govekar, A. Legat, *Corros. Sci.*, 52 (2010) 2015–2025
16. D. Xia, S. Song, J. Wang, J. Shi, H. Bi, Z. Gao, *Electrochem. Commun.*, 15 (2012) 88–92
17. Y. Zhou, D. Mei Luo, *Mater. Charact.*, 62 (2011) 931 – 937
18. H. Saage, M. Krüger, D. Sturm, M. Heilmaier, J.H. Schneibel, E. George, L. Heatherly, Ch. Somsen, G. Eggeler, Y. Yang, *Acta Mater.*, (2009) 3895-3901
19. M. Curionia, R.A. Cottis, M. Di Natale, G.E. Thompson, *Electrochim. Acta.*, 56 (2011) 6318– 6329
20. G. Du, J. Li, W.K. Wang, C. Jiang, S.Z. Song, *Corros. Sci.*, 53 (2011) 2918–2926